

Dwarf galaxies imply dark matter is heavier than 2.2×10^{-21} eV

Tim Zimmermann,^{1,*} James Alvey,^{2,†} David J. E. Marsh,^{3,‡} Malcolm Fairbairn,^{3,§} and Justin I. Read^{4,¶}

¹*Institute of Theoretical Astrophysics, University of Oslo, P.O. Box 1029 Blindern, Oslo, Norway*

²*GRAPPA Institute, Institute for Theoretical Physics Amsterdam,*

University of Amsterdam, Science Park 904, 1098 XH Amsterdam, The Netherlands

³*Theoretical Particle Physics and Cosmology, King's College London, Strand, London, WC2R 2LS, United Kingdom*

⁴*Department of Physics, University of Surrey, Guildford, GU2 7XH, UK*

Folk wisdom dictates that a lower bound on the dark matter particle mass, m , can be obtained by demanding that the de Broglie wavelength in a given galaxy must be smaller than the virial radius of the galaxy, leading to $m \gtrsim 10^{-22}$ eV when applied to typical dwarf galaxies. This lower limit has never been derived precisely or rigorously. We use stellar kinematical data for the Milky Way satellite galaxy Leo II to self-consistently reconstruct a statistical ensemble of dark matter wavefunctions and corresponding density profiles. By comparison to a data-driven, model-independent reconstruction, and using a variant of the maximum mean discrepancy as a statistical measure, we determine that a self-consistent description of dark matter in the local Universe requires $m > 2.2 \times 10^{-21}$ eV (CL > 95%). This lower limit is free of any assumptions pertaining to cosmology, microphysics (including spin), or dynamics of dark matter, and only assumes that it is predominantly composed of a single bosonic particle species.

GitHub: The JAXSP library is available at [timzimm/jaxsp](https://github.com/timzimm/jaxsp). In addition, the scripts to generate the results in this work can be found at [timzimm/boson_dsph](https://github.com/timzimm/boson_dsph).

Introduction. Astrophysical evidence for a large amount of gravitationally interacting matter, which cannot be explained in the context of the Standard Model of particle physics and General Relativity, has been accumulating for more than 100 years [1, 2]. Nonetheless, the identity and precise nature of dark matter (DM) remains one of the biggest questions in our understanding of the Universe. There is a myriad of evidence – coming from, e.g., observations of the cosmic microwave background [3], galaxy clusters (e.g. [4]), large-scale structure (e.g. [5]), or stellar kinematics (e.g. [6]) – for the existence of such a non-baryonic matter component. To date, however, no definitive laboratory or non-gravitational signature has been observed. As such, despite the efforts of direct detection facilities (e.g. [7, 8]), large-scale cosmology surveys [3–5], and telescopes (see Ref. [9] for a review of indirect detection searches), the dark matter parameter space remains wide open.

If dark matter is thought of as dominantly composed of a single particle or composite object, it is natural to categorise DM according to the mass, m , of the constituent. At the highest end, we have macroscopic objects, such as black holes or other massive objects. Dynamical effects of these objects on star clusters, for example, lead to an upper limit on the allowed mass in the range of 10 solar masses (M_\odot) [10]. For $m < M_{\text{Pl}}$, where M_{Pl} is the Planck mass, DM may be composed of a new fundamental particle. For decades, experimental programs have been developed to search for such particles, for example scattering of DM with $m \approx 1$ GeV off atomic nuclei (e.g. [7]), or resonant production of radio waves in microwave cavities for DM with $m \approx 1 \mu\text{eV}$ (e.g. [8]).

In this *Letter* we ask the simple question: what is the smallest value m can possibly take, consistent with kine-

matical considerations? Specifically, we are interested in the implications of kinematical observations of Milky Way dwarf spheroidal galaxies.

If DM is a fermion, then the resulting lower limit is known as the Tremaine-Gunn bound [11]. As a result of the Pauli exclusion principle, fermions cannot multiply occupy states in phase space, and so bounding the distribution function $f \leq 1$, one can estimate a lower limit on m given the mass and radius (and hence virial equilibrium velocity) of a galaxy. Modelling a dwarf galaxy as a homogeneous, spherically symmetric and degenerate Fermi gas with $M \simeq 10^8 M_\odot$ and $R \simeq 1.0$ kpc, this gives an estimated lower bound $m_f \gtrsim 120$ eV [12]. This limit can be improved by accurately reconstructing the phase space distribution function via the observed kinematics of tracer stars hosted by the Milky way dwarfs, which leads to $m_f > 130$ eV at the 95% confidence level (CL) [13]. However, this limit does not apply if DM is a boson.

For a boson, a limit as fundamental as the fermionic Tremaine-Gunn bound can be estimated by invoking the uncertainty principle $m\sigma_v\sigma_r \gtrsim 3/2 \times \hbar$ [14]. For a steady-state, spherically symmetric object like a dwarf galaxy composed of bosonic DM to exist, its spatial extent r_{vir} and characteristic velocity dispersion σ_v must satisfy $m \gtrsim 3/2 \times \hbar (\sigma_v r_{\text{vir}})^{-1}$. If we estimate the virial radius, r_{vir} , and velocity dispersion, σ_v , for the Milky Way dwarf Leo II [15] as $r_{\text{vir}} \simeq 9$ kpc and $\sigma_v \simeq 15$ km s⁻¹ [16, 17],¹

¹ As is customary, we set $r_{\text{vir}} = r_{200}$, i.e. the radius within which the mean density equals 200 times the critical density, and estimate σ_v via the scalar virial theorem [18]: $\sigma_v^2 = 2\pi M_{\text{tot}}^{-1} |\int dr r^2 \rho(r) V(r)|$.

this leads to $m \gtrsim 2 \times 10^{-23}$ eV. This is at the same order of magnitude as the commonly assumed lower limit on the DM particle mass: the ‘folk limit’ referred to in the abstract. In the rest of this *Letter*, we work to derive a more rigorous limit, which will turn out to be two orders of magnitude stronger. In particular, we strengthen the limit to $m > 2.2 \times 10^{-21}$ eV (CL > 95%). Of course, there are a number of other relevant limits on ultra-light dark matter candidates, see in particular Refs. [19–21]. Such limits, however, depend on details of cosmology, non-linear gas physics, and/or long-time dynamics, all of which our limit is independent of. We postpone a detailed comparison and discussion to the end of this work.

Our rigorous analysis is composed of two steps: Starting from the assumption of a stationary and spherically symmetric galaxy, we reconstruct an ensemble of 5000 DM wave functions for Leo II as an exhaustive expansion in DM energy eigenstates, using as input an ensemble of reconstructions of the gravitational potential. We then compare our wave functions to an, effectively model-agnostic, reconstruction of the density profile derived from stellar kinematical data and vary the boson mass m until both ensembles are statistically indistinguishable. We formalise this idea as a non-parametric, two-sample hypothesis test based on the *fused maximum mean discrepancy* [22, 23] for functional data [24]. The analysis relies on JAXSP, our differentiable and scalable wave function reconstruction tool based on a semi-analytical treatment of Schrödinger’s equation. We describe JAXSP in our companion paper [25] (in prep.).

Leo II dSph data. To carry out the wavefunction fit, we require robust data-driven reconstructions of the DM density profiles within dwarf galaxies. Specifically, we need a statistical ensemble of spherically symmetric DM density profiles $\rho(r)$ that are consistent with the photometric and kinematical measurements of the stellar tracer population in Leo II [15]. For this we use GRAVSPHERE [16, 17, 26, 27], a Markov-Chain-Monte-Carlo sampler that infers realisations of ρ by solving the spherical Jeans equation [18, 28, 29]. To mitigate the well-known degeneracy between the halo density and the stellar velocity anisotropy inherent to Jeans modelling [30–33], GRAVSPHERE incorporates higher order velocity moments, so called virial shape parameters [30, 34], into its likelihood. The results of this analysis are posterior parameter samples for the highly flexible, CORENFWTIDES-density model, ρ_{cNFWt} . This density model augments the canonical NFW profile [35] with four additional parameters. At small radii, a ‘coredness’ parameter, $0 \leq n \leq 1$, and core radius r_c permit us to interpolate between a perfect core $\rho(r \ll r_c) \sim \rho_0$ or cusp $\rho(r \ll r_c) \sim r^{-1}$. At large radii, the introduction of a tidal radius r_t and power law decay $\rho(r \gg r_t) \sim r^{-\delta}$ allow for an effective model of tidal forces stripping peripheral mass away, if a larger host halo is present.

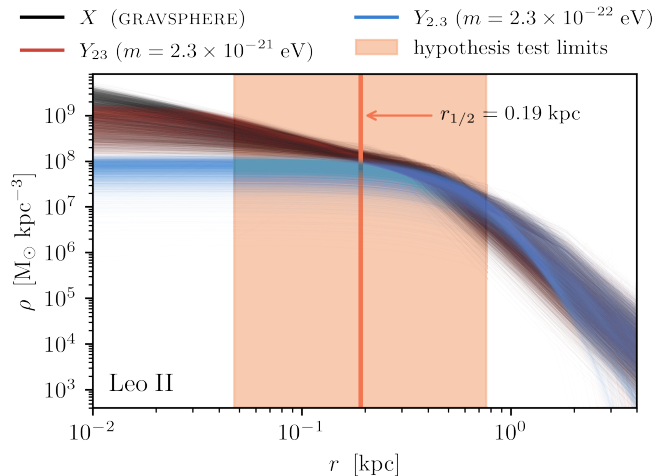


FIG. 1. Direct comparison of different density ensembles for the Milky way dwarf Leo II. Black curves depict density samples generated by the Jeans code GRAVSPHERE and act as data-driven input set X to our analysis pipeline. The pipeline output is a population $Y_{m_{22}}$ of reconstructed DM wave functions densities $\langle |\psi|^2 \rangle$ at boson mass $m = m_{22} \times 10^{-22}$ eV (red/blue curves). Higher mass eigenstates enjoy a stronger spatial localisation, and are therefore able to resolve more structure of a cuspy input density at small radii. Testing this small scale discrepancy in the validity region of GRAVSPHERE (orange sector) at the population level, cf. Fig. 3, summarises the key idea behind our lower mass limit.

Our choice of Leo II was motivated by its ability to set a strong limit due to its steep inner profile, and its statistically robust description as a static [36, 37], spherically symmetric distribution [37–40] with a well measured cusp. Draco is another possible candidate object [41], however, it is computationally more challenging with our method [25]. We have explicitly checked in a pared-down analysis that Draco gives a consistent limit with Leo II.

Fig. 1 displays the 5000 posterior samples for Leo II (black lines) that we use in our analysis. Note that Collins et al. [17] also validate GRAVSPHERE’s mass modelling on the spherical mock data described in Ref. [42]² and find it to recover the true density within the 95% confidence interval of the density samples over the radial range $0.25 \leq r/r_{1/2} \leq 4$ (orange sector in Fig. 1) around the half-light radius $r_{1/2}$ even if only $O(100)$ tracers are available. We adopt this radial range for our analysis.

Self-consistent Reconstruction of the DM wave function. In the non-relativistic limit, the dynamics of spin zero, bosonic DM with $m \ll O(10)$ eV are described by a complex scalar $\psi(\mathbf{x}, t)$ that obeys the Schrödinger-Poisson (SP) equation [43] and sources its gravitational potential V via the DM density $\rho(\mathbf{x}, t) = |\psi(\mathbf{x}, t)|^2$. As-

² Also available as part of the [Gaia Challenge](#)

suming stationary conditions, i.e. no explicit time dependency in ρ and V , and restricting to spherically symmetric objects, the linear set of equations:

$$-\frac{\hbar^2}{2m} \left(\frac{\partial^2}{\partial r^2} - \frac{l(l+1)}{r^2} \right) u_{nl} + mV u_{nl} = E_{nl} u_{nl}, \quad (1)$$

$$\left(\frac{\partial^2}{\partial r^2} + \frac{1}{r} \frac{\partial}{\partial r} \right) V = 4\pi G \rho,$$

with eigenmode $\psi_{nlm}(\mathbf{x}, t) = r^{-1} u_{nl}(r) Y_l^m(\phi, \theta) e^{iE_{nl}t/\hbar}$ has proven to be an effective approximation for the equilibrium phenomena encapsulated in the full-fledged SP equation [44–46].

From a practical perspective, and following Refs. [46, 47], Eq. (1) breaks the non-linear relation between wave function ψ and potential V . In addition, it approximates ρ as a stationary density that is *independent* of the wave function. In this way, Eq. (1) is equivalent to a linear order perturbative treatment of ψ with V as the zeroth-order potential [45].

The full process of this reconstruction of the wave function, described in more detail in our companion paper [25] (in prep.), may be seen as an evolution of the approaches presented in Refs. [46, 47]. Here we recall the main three steps: Firstly, given a density realisation, we compute its time-independent gravitational potential via the Poisson equation. We then compute an extensive (and exhaustive) library of eigenstates that contains all modes u_{nl} with a classically allowed region within r_{99} , i.e. the radius enclosing 99% of the total mass. This involves repeatedly solving Eq. (1) for increasing values of the angular momentum quantum number l — a task we solve in practice by application of a piecewise, perturbative approximation to Eq. (1). We have found this to vastly outperform standard matrix diagonalisation methods [44–46] in terms of accuracy, computational complexity and scalability to higher boson masses m : Reconstructing an eigenstate library with $J = 10^5$ modes with a low order matrix discretisation requires $O(10)$ hrs compared to only $O(1)$ min in our piecewise perturbative approach. Lastly, we establish self-consistency between the density sample ρ_{cNFWt} and the spherically averaged wave function: $\langle |\psi|^2 \rangle = (4\pi r^2)^{-1} \sum_{nl} (2l+1) |a_{nl}|^2 u_{nl}^2(r)$, by minimising an objective function of our choice³ over the mode coefficients $|a_{nl}|$ — in this work the symmetric Jensen-Shannon divergence.⁴

³ We have also explicitly tested different convex objective functions, including the Kullback-Leibler divergence and a mean-squared error function.

⁴ Together with the eigenstate library construction and mode coefficient optimisation, for a single representative mass $m = 2.3 \times 10^{-21}$ eV, our pipeline takes $O(2)$ days to run on 100 CPU cores for 5000 profiles. Alongside this, there is typically a significant memory footprint of $O(2)$ TB when holding the eigenstate libraries in memory during the optimisation step.

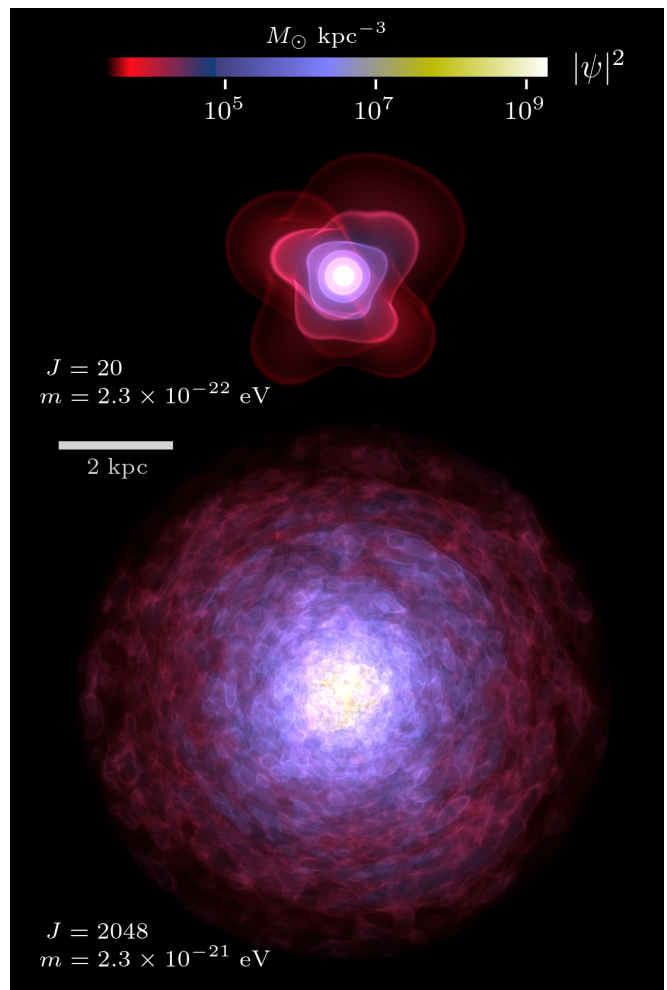


FIG. 2. Volume rendering of the total wave function density $|\psi|^2$ reconstructed from the average profile $\langle \rho_{\text{cNFWt}} \rangle$ of Fig. 1 for an excluded (**top**) and allowed (**bottom**) value of m according to the hypothesis test in Fig. 3. J denotes the total number of radial modes u_{nl} in the eigenstate expansion.

As a concrete example, in Fig. 1 we show the set of reconstructed $\langle |\psi|^2 \rangle$ for the input densities ρ_{cNFWt} from GRAVSPHERE for two different boson masses — $m = 2.3 \times 10^{-22}$ eV (excluded by our analysis) and $m = 2.3 \times 10^{-21}$ eV (not excluded). In Fig. 2, we show the full wave function $|\psi(r, \phi, \theta)|^2 = \langle |\psi|^2 \rangle(r) + \chi(r, \phi, \theta)$, including the interference cross-term χ . The presence of χ induces intriguing physics in its own right and may be used to put constraints on the boson mass. Our limit is derived exclusively from the time independent background contribution $\langle |\psi|^2 \rangle$.

How to exclude boson masses. It is perhaps tempting to incorporate an eigenstate expansion approach into a textbook Jeans analysis, i.e. define a parametrised potential, construct the corresponding eigenstate library, and incorporate $\langle |\psi|^2 \rangle$ into a likelihood to sample the full posterior distribution of the mode coefficients. Un-

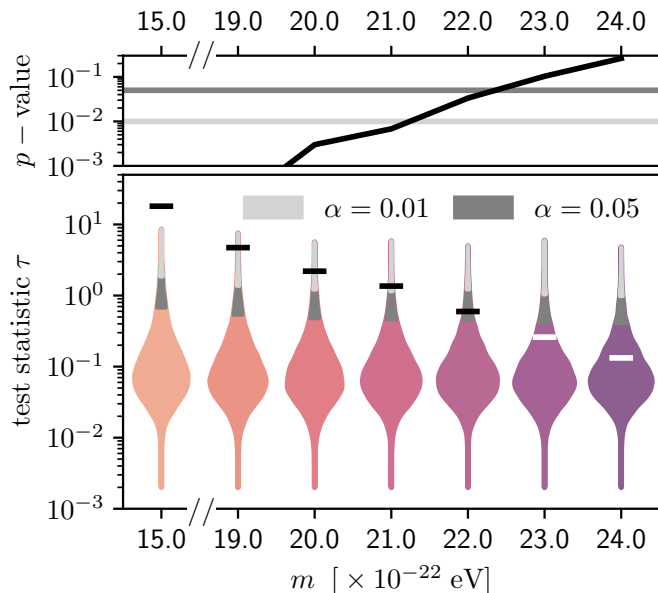


FIG. 3. Non-parametric, two-sample hypothesis test for distribution equality based on the fused maximum mean discrepancy $\tau(Z)$ as test statistic. Shown is the distribution of $\tau(Z)$ under the null hypothesis obtained by a permutation bootstrap. Areas in shades of gray illustrate the rejection regions at significance α . Black/white bars depict the realised value of the test statistic. We determine $m > 2.2 \times 10^{-21}$ eV as the first mass compatible with the null hypothesis at CL $> 95\%$.

fortunately, this is computationally intractable. Depending on the boson mass and depth of the potential well, eigenstate library sizes of $J = \mathcal{O}(10^4 - 10^5)$ are common, rendering standard sampling techniques ineffective.

The question then is how to determine if a given boson mass self-consistently reproduces the true distribution of density profiles as defined by the GRAVSPHERE Jeans analysis. In order to answer this question, we construct a non-parametric, two-sample hypothesis test that ascertains whether the set of GRAVSPHERE functions, $X = \{\rho_{\text{cNFWt},j}\}_{j=1}^{5000}$, and the set of wavefunction densities for boson mass m , $Y_m = \{|\psi|^2_j\}_{j=1}^{5000}$, are drawn from the same underlying distribution. Our null hypothesis is therefore $H_0 : p = q_m$, where we denote p as the “posterior distribution over density profiles consistent with Leo II stellar kinematic data” and q_m as “the corresponding distribution of reconstructed density profiles for a fixed boson mass m ”. Our (lower) limit on m at confidence level (CL) $(1 - \alpha)$ is then obtained once the null hypothesis cannot be rejected at the α significance level. Intuitively, this happens at a mass with eigenstate libraries flexible enough to recover all of the GRAVSPHERE densities equally well, irrespective of whether they are cored or cusped.

There are two technical hurdles that we need to overcome to apply this test in practice. Firstly, we need to define a test statistic $\tau(X_1, X_2)$ over two samples of den-

sity profiles, $X_{1,2}$. Secondly, at a given boson mass m , we need to derive the distribution of τ under the null hypothesis, $p(\tau | H_0)$, where $X_{1,2}$ are both drawn from the same distribution. With this, we can then evaluate the test statistic on the “observed” samples $\tau_o = \tau(X, Y_m)$ and compare it to the critical values of the distribution $p(\tau | H_0)$ at the desired significance level.

In this work, we use an estimator for the *fused maximum mean discrepancy* (MMD) as a test statistic [22–24, 48].⁵ We refer to the *Supplemental Material* for full technical details, however, it can be shown that MMD constitutes a metric on the space of probability distributions and that $\tau(X, Y_m) \xrightarrow{N \rightarrow \infty} \text{MMD}(p, q_m)$, thus providing an intuitive “distance-based” interpretation for τ . As such, we can reject H_0 under the observation of sufficiently *large* values of τ_o .

With the test statistic chosen, we follow Ref. [23] and compute $p(\tau | H_0)$ by using a permutation resampling, i.e. we randomly shuffle the combined set $Z = (X, Y_m)$ (mixing GRAVSPHERE and wavefunction densities), split into two equal parts, $X_1 \cup X_2 = Z$, and compute $\tau(X_1, X_2)$. We repeat this process $\mathcal{O}(10^5)$ times to obtain an empirical estimate of the cumulative distribution (CDF) of $p(\tau | H_0)$ and reject H_0 if the observed value of τ_o exceeds the $(1 - \alpha)$ quantile of the CDF (this sampling is conservative [49], which we have verified by comparing to the distribution obtained using only the GRAVSPHERE functions). A more intuitive example of this test applied to the coredness parameter in the CORENFWTIDES profile is provided in the appendix.

Results. Fig. 3 depicts the distribution of the test statistic τ under the null hypothesis H_0 , and the critical values of this distribution at the $\alpha = 1\%, 5\%$ levels. For a set of boson masses $m \in [15, 24] \times 10^{-22}$ eV, we evaluate the test statistic τ_o (shown by the black/white horizontal lines in the figure) and compare them to the critical values of the distribution. As expected, we see that at larger masses, τ_o is fully consistent with the distribution under H_0 . In this regime, the reconstructed wavefunctions are statistically indistinguishable from the GRAVSPHERE density profiles. On the other hand, at low masses, the eigenstate superposition is unable to reproduce key features (in particular the cuspiest profiles) across the samples, translating into a statistical discrepancy and rejection of H_0 .

The key result of this work is that we find $m > 2.2 \times 10^{-21}$ eV (CL $> 95\%$). This result is largely unaffected by moderate changes of the radial range on which the hypothesis test is conducted. Also, evaluating the two-

⁵ In the context of two-sample, distribution equality testing, [23] benchmark the fused maximum mean discrepancy against a selection of state-of-the-art test statistics, and find it to be on par or outperform them in terms correctly rejecting H_0 .

body relaxation rate at this mass gives a timescale much longer than the age of the Universe [50], making it fully consistent with our modeling of Leo II as stationary.

Our robust lower limit on the DM mass is two orders of magnitude stronger compared to a naive estimate based on the uncertainty principle. The reported improvement may be intuitively understood as a consequence of applying the uncertainty condition at the level of individual eigenstates rather than at the level of the overall wave function: Each eigenstate, ψ_j , has a spatial extent set by its uncertainty $\sigma_r^2 = \langle \psi_j | r^2 | \psi_j \rangle - \langle \psi_j | r | \psi_j \rangle^2$ and thus contributes to the dwarf density at that particular length scale. The inferred Leo II DM density is cuspy, i.e. well modeled by a steep power law, on certain length scales. If the length scale of this cusp is comparable to the position uncertainty σ_r of the wavefunction, then the eigenstate expansion will not be able to adequately reproduce the density profile. To compensate, the spatial extent of all modes must shrink, requiring an increased boson mass m , and tightening the lower limit. If the dark matter distribution would be cored, a lower mass would suffice to reproduce the density ensemble at small radii. We checked this explicitly by applying our analysis to Fornax [51] yielding a weakened limit of $m > 4 \times 10^{-22}$ eV (broadly consistent with related studies [33, 52]).

Significance and generality of the result. There are, of course, many other lower limits on the DM mass that rely on similar physics to that which has been used in this work. We mention a few here for comparison. If the DM relic density arises from coherent motion in a harmonic potential, then the cosmic microwave background anisotropies constrain $m > 10^{-24}$ eV [53], which is improved to $m > 10^{-23}$ eV with weak gravitational lensing [54] and to $m > 2 \times 10^{-20}$ eV including modeling of intergalactic gas in the Lyman-alpha forest [19]. The same cosmological models can be used to make predictions about galaxy number counts, e.g. Ref. [55] finds $m > 2.9 \times 10^{-21}$ eV in order to produce the abundance of satellite galaxies of the Milky Way, while Ref. [56] finds $m > 2.5 \times 10^{-22}$ eV to explain high redshift galaxies observed by Hubble and James Webb space telescopes. All of these lower limits are less generic than ours since they rely on assumptions about cosmology and/or complex non-linear dynamics.

In addition, the physics of the SP system gives rise to a rich phenomenology of nonlinear wave effects [57]. Dynamical heating of the stellar tracer population [50] in Eridanus-II leads to the lower limit $m > 3 \times 10^{-19}$ eV [20, 21]. This limit is less fundamental than ours, since it relies on dynamics over billions of years (it is dynamical, rather than kinematical), and could be strongly affected by unmodeled events in the history of the galaxy.

We computed our lower limit for a boson with spin $s = 0$. Higher spin bosonic DM is also of interest (see e.g. Ref. [58]). In such a case, there are copies of the DM wave

function for each polarisation state. Taking the superposition of such terms to form the total density reduces the amplitude of the interference term $\chi(r, \phi, \theta)$, but does not affect the spherically averaged density $\langle |\psi^2| \rangle$ [59–61]. Thus our lower limit applies equally to $s = 0$ and to higher spin DM.

There are a number of studies of the Milky Way satellites and other galaxies, which attempt to fit a model inspired by the behaviour of ultralight bosons, namely an outer power-law piece, with an inner solitonic core [57]. The amplitude of the ground state wavefunction in our analysis effectively accounts for the presence of a soliton with an arbitrary “core-halo” relation [62, 63] (displacement of the soliton from the halo centre in simulations is small [64] and should not affect our spherical halo assumption). For example, Refs. [33, 57, 65–70] also use Jeans analysis or simplifications thereof, while Ref. [71] fits rotation curves. All of these works find *preferred* values of m that fit the cored density profiles of certain galaxies. When taken globally, the smallest cores lead to results that are in tension with the observed masses of larger galaxies, leading to lower limits or very large preferred values for m as in Refs. [68–70]. It is well known, however, that cores can be explained by other physics, such as stellar heating [72]. For the first time in this context, we used a fully self-consistent density profile comprised of energy eigenstates instead of the heuristic composite, and thus our limit is unaffected by uncertainties on the “core-halo” relation [63]. In essence, our robust limit comes down to fitting the inner slope of a non-cored object, which is therefore also unaffected by any baryonic physics that may lead to cores in other galaxies.

Conclusions. We have developed a robust and advanced methodology, both computationally and statistically, to set the strongest *fundamental* lower limit to date on the DM particle mass, $m > 2.2 \times 10^{-21}$ eV. Our methodology could be extended in future to constrain the fraction of DM with $m < 2.2 \times 10^{-21}$ eV by including an additional cold component in the gravitational potential. Such constraints on mixed DM may be competitive with cosmological bounds, and if accurate to $\mathcal{O}(10\%)$ may probe interesting high energy physics models [52, 73]. This would also relax the only assumption about the composition of DM in our analysis.

ACKNOWLEDGEMENTS

We acknowledge useful conversations with Valerie Domcke, Miguel Escudero, Sebastian Hoof, Jens Niemeyer, and Hans Winther. The authors would like to thank Charis Pooni for collaboration at an early stage of the development of JAXSP. TZ acknowledges funding from the European Union’s Horizon 2020 research and innovation programme under the Marie Skłodowska-Curie grant agreement No. 945371 and support through a Kris-

tine Bonnevie travel grant (University of Oslo). JA acknowledges funding from the European Research Council (ERC) under the European Union’s Horizon 2020 research and innovation programme (Grant agreement No. 864035). DJEM is supported by an Ernest Rutherford Fellowship from the STFC, Grant No. ST/T004037/1 and by a Leverhulme Trust Research Project (RPG-2022-145). MF was supported by the United Kingdom STFC Grants ST/T000759/1 and ST/T00679X/1. JIR would like to thank the STFC for support from grants ST/Y002865/1 and ST/Y002857/1.

* timzi@astro.uio.no

† j.b.g.alvey@uva.nl

‡ david.j.marsh@kcl.ac.uk

§ malcolm.fairbairn@kcl.ac.uk

¶ j.read@surrey.ac.uk

- [1] G. Bertone and D. Hooper, History of dark matter, *Rev. Mod. Phys.* **90**, 045002 (2018), [arXiv:1605.04909](https://arxiv.org/abs/1605.04909) [astro-ph.CO].
- [2] D. J. E. Marsh, D. Ellis, and V. M. Mehta, *Dark Matter: Evidence, Theory, and Constraints* (Princeton University Press, 2024).
- [3] N. Aghanim *et al.* (Planck), Planck 2018 results. VI. Cosmological parameters, *Astron. Astrophys.* **641**, A6 (2020), [Erratum: *Astron. Astrophys.* 652, C4 (2021)], [arXiv:1807.06209](https://arxiv.org/abs/1807.06209) [astro-ph.CO].
- [4] S. Alam *et al.* (BOSS), The clustering of galaxies in the completed SDSS-III Baryon Oscillation Spectroscopic Survey: cosmological analysis of the DR12 galaxy sample, *Mon. Not. Roy. Astron. Soc.* **470**, 2617 (2017), [arXiv:1607.03155](https://arxiv.org/abs/1607.03155) [astro-ph.CO].
- [5] D. J. Eisenstein *et al.* (SDSS), Detection of the Baryon Acoustic Peak in the Large-Scale Correlation Function of SDSS Luminous Red Galaxies, *Astrophys. J.* **633**, 560 (2005), [arXiv:astro-ph/0501171](https://arxiv.org/abs/astro-ph/0501171).
- [6] G. Battaglia, A. Helmi, E. Tolstoy, M. Irwin, V. Hill, and P. Jablonka, The kinematic status and mass content of the Sculptor dwarf spheroidal galaxy, *Astrophys. J. Lett.* **681**, L13 (2008), [arXiv:0802.4220](https://arxiv.org/abs/0802.4220) [astro-ph].
- [7] E. Aprile *et al.* (XENON), Dark Matter Search Results from a One Ton-Year Exposure of XENON1T, *Phys. Rev. Lett.* **121**, 111302 (2018), [arXiv:1805.12562](https://arxiv.org/abs/1805.12562) [astro-ph.CO].
- [8] C. Bartram *et al.* (ADMX), Search for Invisible Axion Dark Matter in the 3.3–4.2 μeV Mass Range, *Phys. Rev. Lett.* **127**, 261803 (2021), [arXiv:2110.06096](https://arxiv.org/abs/2110.06096) [hep-ex].
- [9] J. M. Gaskins, A review of indirect searches for particle dark matter, *Contemp. Phys.* **57**, 496 (2016), [arXiv:1604.00014](https://arxiv.org/abs/1604.00014) [astro-ph.HE].
- [10] T. D. Brandt, Constraints on MACHO Dark Matter from Compact Stellar Systems in Ultra-Faint Dwarf Galaxies, *Astrophys. J. Lett.* **824**, L31 (2016), [arXiv:1605.03665](https://arxiv.org/abs/1605.03665) [astro-ph.GA].
- [11] S. Tremaine and J. E. Gunn, Dynamical Role of Light Neutral Leptons in Cosmology, *Phys. Rev. Lett.* **42**, 407 (1979).
- [12] A. Boyarsky, O. Ruchayskiy, and D. Iakubovskiy, A lower bound on the mass of dark matter particles, *J. Cosmol-ogy Astropart. Phys.* **2009**, 005 (2009), [arXiv:0808.3902](https://arxiv.org/abs/0808.3902) [hep-ph].
- [13] J. Alvey, N. Sabti, V. Tiki, D. Blas, K. Bondarenko, A. Boyarsky, M. Escudero, M. Fairbairn, M. Orkney, and J. I. Read, New constraints on the mass of fermionic dark matter from dwarf spheroidal galaxies, *Mon. Not. Roy. Astron. Soc.* **501**, 1188 (2021), [arXiv:2010.03572](https://arxiv.org/abs/2010.03572) [hep-ph].
- [14] Ł. Rudnicki, Heisenberg uncertainty relation for position and momentum beyond central potentials, *Phys. Rev. A* **85**, 022112 (2012), [arXiv:1112.5198](https://arxiv.org/abs/1112.5198) [quant-ph].
- [15] M. E. Spencer, M. Mateo, M. G. Walker, E. W. Olszewski, A. W. McConnachie, E. N. Kirby, and A. Koch, The Binary Fraction of Stars in Dwarf Galaxies: The Case of Leo II, *AJ* **153**, 254 (2017), [arXiv:1706.04184](https://arxiv.org/abs/1706.04184) [astro-ph.GA].
- [16] J. I. Read and P. Steger, How to break the density-anisotropy degeneracy in spherical stellar systems, *MNRAS* **471**, 4541 (2017), [arXiv:1701.04833](https://arxiv.org/abs/1701.04833) [astro-ph.GA].
- [17] M. L. M. Collins, J. I. Read, R. A. Ibata, R. M. Rich, N. F. Martin, J. Peñarrubia, S. C. Chapman, E. J. Tollerud, and D. R. Weisz, Andromeda XXI - a dwarf galaxy in a low-density dark matter halo, *MNRAS* **505**, 5686 (2021), [arXiv:2102.11890](https://arxiv.org/abs/2102.11890) [astro-ph.GA].
- [18] J. Binney and S. Tremaine, *Galactic dynamics* (1987).
- [19] K. K. Rogers and H. V. Peiris, Strong Bound on Canonical Ultralight Axion Dark Matter from the Lyman-Alpha Forest, *Phys. Rev. Lett.* **126**, 071302 (2021), [arXiv:2007.12705](https://arxiv.org/abs/2007.12705) [astro-ph.CO].
- [20] D. J. E. Marsh and J. C. Niemeyer, Strong Constraints on Fuzzy Dark Matter from Ultrafaint Dwarf Galaxy Eridanus II, *Phys. Rev. Lett.* **123**, 051103 (2019), [arXiv:1810.08543](https://arxiv.org/abs/1810.08543) [astro-ph.CO].
- [21] N. Dalal and A. Kravtsov, Excluding fuzzy dark matter with sizes and stellar kinematics of ultrafaint dwarf galaxies, *Phys. Rev. D* **106**, 063517 (2022).
- [22] A. Gretton, K. M. Borgwardt, M. J. Rasch, B. Schölkopf, and A. Smola, A kernel two-sample test, *Journal of Machine Learning Research* **13**, 723 (2012).
- [23] F. Biggs, A. Schrab, and A. Gretton, MMD-FUSE: Learning and combining kernels for two-sample testing without data splitting, *Advances in Neural Information Processing Systems* **36** (2023), [arXiv:2306.08777](https://arxiv.org/abs/2306.08777) [stat.ML].
- [24] G. Wynne and A. B. Duncan, A Kernel Two-Sample Test for Functional Data, *arXiv e-prints*, [arXiv:2008.11095](https://arxiv.org/abs/2008.11095) (2020), [arXiv:2008.11095](https://arxiv.org/abs/2008.11095) [math.ST].
- [25] T. Zimmermann, J. Alvey, D. Marsh, and M. Fairbairn, *jaxsp*: A new code for self-consistently solving the Schrödinger-Poisson equations (*to appear*), (2024), [arXiv:2407.xxxx](https://arxiv.org/abs/2407.xxxx) [astro-ph.CO].
- [26] J. I. Read, M. G. Walker, and P. Steger, The case for a cold dark matter cusp in Draco, *MNRAS* **481**, 860 (2018), [arXiv:1805.06934](https://arxiv.org/abs/1805.06934) [astro-ph.GA].
- [27] A. Genina, J. I. Read, C. S. Frenk, S. Cole, A. Benítez-Llambay, A. D. Ludlow, J. F. Navarro, K. A. Oman, and A. Robertson, To β or not to β : can higher order Jeans analysis break the mass-anisotropy degeneracy in simulated dwarfs?, *MNRAS* **498**, 144 (2020), [arXiv:1911.09124](https://arxiv.org/abs/1911.09124) [astro-ph.GA].
- [28] J. H. Jeans, The Motions of Stars in a Kapteyn Universe, *MNRAS* **82**, 122 (1922).
- [29] J. Binney and G. A. Mamon, M/L and velocity anisotropy from observations of spherical galaxies, or

- must M87 have a massive black hole?, *MNRAS* **200**, 361 (1982).
- [30] M. R. Merrifield and S. M. Kent, Fourth Moments and the Dynamics of Spherical Systems, *AJ* **99**, 1548 (1990).
- [31] M. I. Wilkinson, J. Kleyna, N. W. Evans, and G. Gilmore, Dark matter in dwarf spheroidals - I. Models, *MNRAS* **330**, 778 (2002), [arXiv:astro-ph/0109451 \[astro-ph\]](#).
- [32] E. L. Lokas and G. A. Mamon, Dark matter distribution in the Coma cluster from galaxy kinematics: breaking the mass-anisotropy degeneracy, *MNRAS* **343**, 401 (2003), [arXiv:astro-ph/0302461 \[astro-ph\]](#).
- [33] A. X. González-Morales, D. J. E. Marsh, J. Peñarrubia, and L. A. Ureña-López, Unbiased constraints on ultralight axion mass from dwarf spheroidal galaxies, *MNRAS* **472**, 1346 (2017), [arXiv:1609.05856 \[astro-ph.CO\]](#).
- [34] T. Richardson and M. Fairbairn, On the dark matter profile in Sculptor: breaking the β degeneracy with Virial shape parameters, *MNRAS* **441**, 1584 (2014), [arXiv:1401.6195 \[astro-ph.GA\]](#).
- [35] J. F. Navarro, C. S. Frenk, and S. D. M. White, A Universal Density Profile from Hierarchical Clustering, *ApJ* **490**, 493 (1997), [arXiv:astro-ph/9611107 \[astro-ph\]](#).
- [36] J. I. Read, M. I. Wilkinson, N. W. Evans, G. Gilmore, and J. T. Kleyna, The importance of tides for the Local Group dwarf spheroidals, *MNRAS* **367**, 387 (2006), [arXiv:astro-ph/0511759 \[astro-ph\]](#).
- [37] M. De Leo, J. I. Read, N. E. D. Noel, D. Erkal, P. Masana, and R. Carrera, Surviving the Waves: evidence for a Dark Matter cusp in the tidally disrupting Small Magellanic Cloud, [arXiv e-prints](#), [arXiv:2303.08838 \(2023\)](#), [arXiv:2303.08838 \[astro-ph.GA\]](#).
- [38] J. I. Read and P. Steger, How to break the density-anisotropy degeneracy in spherical stellar systems, *MNRAS* **471**, 4541 (2017), [arXiv:1701.04833 \[astro-ph.GA\]](#).
- [39] J. I. Read, M. G. Walker, and P. Steger, The case for a cold dark matter cusp in Draco, *MNRAS* **481**, 860 (2018), [arXiv:1805.06934 \[astro-ph.GA\]](#).
- [40] A. Genina, J. I. Read, C. S. Frenk, S. Cole, A. Benítez-Llambay, A. D. Ludlow, J. F. Navarro, K. A. Oman, and A. Robertson, To β or not to β : can higher order Jeans analysis break the mass-anisotropy degeneracy in simulated dwarfs?, *MNRAS* **498**, 144 (2020), [arXiv:1911.09124 \[astro-ph.GA\]](#).
- [41] A. Alvarez, F. Calore, A. Genina, J. Read, P. D. Serpico, and B. Zaldivar, Dark matter constraints from dwarf galaxies with data-driven J-factors, *JCAP* **2020** (9), 004, [arXiv:2002.01229 \[astro-ph.HE\]](#).
- [42] J. I. Read, G. A. Mamon, E. Vasiliev, L. L. Watkins, M. G. Walker, J. Peñarrubia, M. Wilkinson, W. Dehnen, and P. Das, Breaking beta: a comparison of mass modelling methods for spherical systems, *MNRAS* **501**, 978 (2021), [arXiv:2011.09493 \[astro-ph.GA\]](#).
- [43] L. Hui, Wave Dark Matter, *ARA&A* **59**, 247 (2021), [arXiv:2101.11735 \[astro-ph.CO\]](#).
- [44] S.-C. Lin, H.-Y. Schive, S.-K. Wong, and T. Chiueh, Self-consistent construction of virialized wave dark matter halos, *Phys. Rev. D* **97**, 103523 (2018), [arXiv:1801.02320 \[astro-ph.CO\]](#).
- [45] N. Dalal, J. Bovy, L. Hui, and X. Li, Don't cross the streams: caustics from fuzzy dark matter, *J. Cosmology Astropart. Phys.* **2021**, 076 (2021), [arXiv:2011.13141 \[astro-ph.CO\]](#).
- [46] T. D. Yavetz, X. Li, and L. Hui, Construction of wave dark matter halos: Numerical algorithm and analytical constraints, *Phys. Rev. D* **105**, 023512 (2022), [arXiv:2109.06125 \[astro-ph.CO\]](#).
- [47] S.-C. Lin, H.-Y. Schive, S.-K. Wong, and T. Chiueh, Self-consistent construction of virialized wave dark matter halos, *Phys. Rev. D* **97**, 103523 (2018), [arXiv:1801.02320 \[astro-ph.CO\]](#).
- [48] B. K. Sriperebudur, A. Grewton, K. Fukumizu, B. Schölkopf, and G. R. G. Lanckriet, Hilbert space embeddings and metrics on probability measures, (2009), [arXiv:0907.5309 \[stat.ML\]](#).
- [49] J. Hemerik and J. Goeman, Exact testing with random permutations, *TEST* **27**, 811 (2018).
- [50] L. Hui, J. P. Ostriker, S. Tremaine, and E. Witten, Ultralight scalars as cosmological dark matter, *Phys. Rev. D* **95**, 043541 (2017), [arXiv:1610.08297 \[astro-ph.CO\]](#).
- [51] M. G. Walker, M. Mateo, and E. W. Olszewski, Stellar Velocities in the Carina, Fornax, Sculptor, and Sextans dSph Galaxies: Data From the Magellan/MMFS Survey, *AJ* **137**, 3100 (2009), [arXiv:0811.0118 \[astro-ph\]](#).
- [52] D. J. E. Marsh, Axion Cosmology, *Phys. Rept.* **643**, 1 (2016), [arXiv:1510.07633 \[astro-ph.CO\]](#).
- [53] R. Hlozek, D. Grin, D. J. E. Marsh, and P. G. Ferreira, A search for ultralight axions using precision cosmological data, *Phys. Rev. D* **91**, 103512 (2015), [arXiv:1410.2896 \[astro-ph.CO\]](#).
- [54] M. Dentler, D. J. E. Marsh, R. Hlozek, A. Laguë, K. K. Rogers, and D. Grin, Fuzzy dark matter and the Dark Energy Survey Year 1 data, *Mon. Not. Roy. Astron. Soc.* **515**, 5646 (2022), [arXiv:2111.01199 \[astro-ph.CO\]](#).
- [55] E. O. Nadler *et al.* (DES), Milky Way Satellite Census. III. Constraints on Dark Matter Properties from Observations of Milky Way Satellite Galaxies, *Phys. Rev. Lett.* **126**, 091101 (2021), [arXiv:2008.00022 \[astro-ph.CO\]](#).
- [56] H. Winch, K. K. Rogers, R. Hlozek, and D. J. E. Marsh, High-redshift, small-scale tests of ultralight axion dark matter using Hubble and Webb galaxy UV luminosities, (2024), [arXiv:2404.11071 \[astro-ph.CO\]](#).
- [57] H.-Y. Schive, T. Chiueh, and T. Broadhurst, Cosmic structure as the quantum interference of a coherent dark wave, *Nature Physics* **10**, 496 (2014), [arXiv:1406.6586 \[astro-ph.GA\]](#).
- [58] M. Jain and M. A. Amin, Polarized solitons in higher-spin wave dark matter, *Phys. Rev. D* **105**, 056019 (2022), [arXiv:2109.04892 \[hep-th\]](#).
- [59] M. A. Amin, M. Jain, R. Karur, and P. Mocz, Small-scale structure in vector dark matter, *JCAP* **08** (08), 014, [arXiv:2203.11935 \[astro-ph.CO\]](#).
- [60] M. Jain, M. A. Amin, J. Thomas, and W. Wanichwecharungruang, Kinetic relaxation and Bose-star formation in multicomponent dark matter, *Phys. Rev. D* **108**, 043535 (2023), [arXiv:2304.01985 \[astro-ph.CO\]](#).
- [61] J. Chen, X. Du, M. Zhou, A. Benson, and D. J. E. Marsh, Gravitational Bose-Einstein condensation of vector or hidden photon dark matter, *Phys. Rev. D* **108**, 083021 (2023), [arXiv:2304.01965 \[astro-ph.HE\]](#).
- [62] H.-Y. Schive, M.-H. Liao, T.-P. Woo, S.-K. Wong, T. Chiueh, T. Broadhurst, and W. Y. P. Hwang, Understanding the Core-Halo Relation of Quantum Wave Dark Matter from 3D Simulations, *Phys. Rev. Lett.* **113**, 261302 (2014), [arXiv:1407.7762 \[astro-ph.GA\]](#).
- [63] H. Y. J. Chan, E. G. M. Ferreira, S. May, K. Hayashi, and M. Chiba, The diversity of core-halo structure in the fuzzy dark matter model, *Mon. Not. Roy. Astron. Soc.* **511**, 943 (2022), [arXiv:2110.11882 \[astro-ph.CO\]](#).

- [64] H.-Y. Schive, T. Chiueh, and T. Broadhurst, Soliton Random Walk and the Cluster-Stripping Problem in Ultra-light Dark Matter, *Phys. Rev. Lett.* **124**, 201301 (2020), [arXiv:1912.09483 \[astro-ph.GA\]](#).
- [65] D. J. E. Marsh and A.-R. Pop, Axion dark matter, solitons and the cusp-core problem, *MNRAS* **451**, 2479 (2015), [arXiv:1502.03456 \[astro-ph.CO\]](#).
- [66] E. Calabrese and D. N. Spergel, Ultra-light dark matter in ultra-faint dwarf galaxies, *MNRAS* **460**, 4397 (2016), [arXiv:1603.07321 \[astro-ph.CO\]](#).
- [67] S.-R. Chen, H.-Y. Schive, and T. Chiueh, Jeans analysis for dwarf spheroidal galaxies in wave dark matter, *MNRAS* **468**, 1338 (2017), [arXiv:1606.09030 \[astro-ph.GA\]](#).
- [68] M. Safarzadeh and D. N. Spergel, Ultra-light Dark Matter is Incompatible with the Milky Way's Dwarf Satellites, (2019), [arXiv:1906.11848 \[astro-ph.CO\]](#).
- [69] I. S. Goldstein, S. M. Koushiappas, and M. G. Walker, Viability of ultralight bosonic dark matter in dwarf galaxies, *Phys. Rev. D* **106**, 063010 (2022), [arXiv:2206.05244 \[astro-ph.GA\]](#).
- [70] K. Hayashi, E. G. M. Ferreira, and H. Y. J. Chan, Narrowing the Mass Range of Fuzzy Dark Matter with Ultrafaint Dwarfs, *ApJ* **912**, L3 (2021), [arXiv:2102.05300 \[astro-ph.CO\]](#).
- [71] N. Bar, D. Blas, K. Blum, and S. Sibiryakov, Galactic rotation curves versus ultralight dark matter: Implications of the soliton-host halo relation, *Phys. Rev. D* **98**, 083027 (2018), [arXiv:1805.00122 \[astro-ph.CO\]](#).
- [72] A. Pontzen and F. Governato, Cold dark matter heats up, *Nature* **506**, 171 (2014), [arXiv:1402.1764 \[astro-ph.CO\]](#).
- [73] A. Arvanitaki, S. Dimopoulos, S. Dubovsky, N. Kaloper, and J. March-Russell, String Axiverse, *Phys. Rev. D* **81**, 123530 (2010), [arXiv:0905.4720 \[hep-th\]](#).

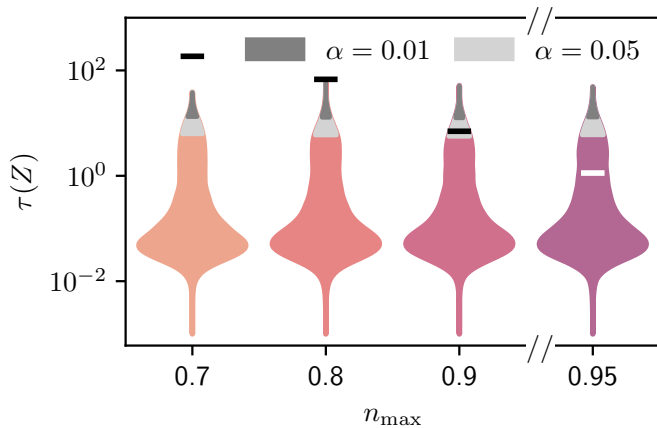


FIG. 4. Two-sample test run on the mock densities in Eq. (2). This test emulates the fully fledged analysis of the main text by replacing the effective $m \rightarrow n(m)$ mapping with a uniform prior $U(0, n_{\max})$ on the coredness parameter n . We find Y to be indistinguishable from X at significance $\alpha = 0.05$ once $n_{\max} = 0.95$.

Technical Appendix: Hypothesis Test Details.

Here, we summarise the details regarding the hypothesis test used in the main text. From a technical perspective, the idea is to (i) identify a metric d on the space $\mathcal{P}(\mathcal{X})$ of probability densities over functions on \mathcal{X} ⁶, $d : \mathcal{P}(\mathcal{X}) \times \mathcal{P}(\mathcal{X}) \rightarrow \mathbb{R}$ and (ii) use an estimator for this distance measure as test statistic.

A suitable candidate for the metric, and the one we adopt in this work, is the *maximum mean discrepancy*, $\text{MMD}(p_x, p_y) = \sup_{f \in \mathcal{F}} |\mathbb{E}_{p_x}(f(x)) - \mathbb{E}_{p_y}(f(y))|$, over a, yet unspecified, class of functionals $\mathcal{F} = \{f : \mathcal{X} \rightarrow \mathbb{R}\}$. A variety of classes is conceivable as discussed in Ref. [48]⁷. Our specific choice is guided by two requirements: On one hand, we demand that MMD is indeed a metric, and thus in particular that $\text{MMD}(p_x, p_y) = 0 \Rightarrow p_x = p_y$. On the other hand, we require that an unbiased estimator for the MMD is easily computable. The authors of [22] advocate to fix a kernel function $k : \mathcal{X} \times \mathcal{X} \rightarrow \mathbb{R}$ and choose its reproducing kernel Hilbert space over \mathcal{X} as the function class over which MMD is computed. In accordance with our preconditions on \mathcal{F} , one can show [22] that

with this choice the intractable optimisation step over \mathcal{F} is eliminated since $\text{MMD}_k(p_x, p_y)^2 = \mathbb{E}_{p_x}[k(x, x')] - 2\mathbb{E}_{p_x, p_y}[k(x, y)] + \mathbb{E}_{p_y}[k(y, y')]$ — now void of any maximisation. Moreover, if we fix $k_\gamma(x, y) = \exp(-\gamma\|x - y\|_{\mathcal{X}}^2)$ as our kernel, Ref. [24] proves that $\text{MMD}_{k_\gamma}(p_x, p_y)$ indeed constitutes a metric on $\mathcal{P}(\mathcal{X})$.

If we let Z be the pair (X, Y) , then a low variance, unbiased estimator $\widehat{\text{MMD}}_{k_\gamma}(Z)$, is given in Refs. [22, 23]. To circumvent data-splitting, we fix the kernel bandwidth γ as proposed and tested in Ref. [23]: instead of using only one heuristically deduced bandwidth, we deploy a selection of prior bandwidths γ_n between $\min d_{ij}$ and $\max d_{ij}$ where the distance matrix element $d_{ij} = \|z_i - z_j\|_{\mathcal{X}}$ and $z_i, z_j \in Z$. Each bandwidth produces a different estimate $\widehat{\text{MMD}}_{k_{\gamma_n}}$ and we fuse them into a consensus statistic $\tau(Z)$ by taking their soft maximum via $\tau(Z) = \log \left[\sum_n \exp \left(\widehat{\text{MMD}}_{k_{\gamma_n}}(Z) \right) \right]$.

Example: Coredness parameter. It is useful to build some intuition for the interpretation of our two-sample hypothesis test. Looking at the exemplary wave functions in Fig. 1, it is apparent that our reconstruction scheme is effectively equivalent to a mapping, $m \rightarrow n(m)$, from boson mass m to the “coredness” parameter n of the CORENFWTIDES profile. This is because, irrespective of the boson mass in the figure, we can fit the NFW tail equally well. We may therefore gain additional insight into the sensitivity of the result presented in the main text by running the two-sample test on:

$$\begin{aligned} X &= \{\rho_{\text{cNFWt},i}(n_i) \mid n_i \sim U(0, 1)\}_{i=1}^{5000}, \\ Y &= \{\rho_{\text{cNFWt},i}(n_i) \mid n_i \sim U(0, n_{\max})\}_{i=1}^{5000}, \end{aligned} \quad (2)$$

with $0 < n_{\max} < 1$ and all other parameters fixed to their original values provided by GRAVSPHERE. Fig. 4 shows the distribution of $\tau(Z)$ for increasing values of n_{\max} .

We find $n_{\max} \geq 0.95$ to be accepted at a significance $\alpha = 0.05$. This simple example motivates the intuitive interpretation of our hypothesis test in terms of detecting statistical discrepancies between sets of overlapping density profiles in the inner region of the dwarf.

⁶ This should be thought of as distributions on function space over square integrable functions defined on the spherical shell $\mathcal{X} = L^2(\mathbb{S}(r_{\min}, r_{\max}))$. Here $r_{\min, \max}$ are set by the validity region

of the GRAVSPHERE posterior (orange sector in Fig. 1).
⁷ For instance, if $X = \mathbb{R}$ and $\mathcal{F} = \{\mathbb{1}_{(-\infty, t]} : t \in \mathbb{R}\}$, the set of indicator functions, one recovers the well-known Kolmogorov distance and the Kolmogorov-Smirnov statistic as its estimator.